# COMPARATIVE STUDY OF ROBUST CONTROL TECHNIQUES FOR OTTO-CYCLE MOTOR CONTROL

**Marcos Salazar Francisco, marcos.salazar@member.isa.org**
**Karl Heinz Kienitz, kienitz@ieee.org**
Instituto Tecnológico da Aeronautica – ITA

***Abstract.*** *This paper compares some aspects of the robust control techniques LQG/LTR and H-∞. These techniques are used to design a multivariable compensator for an old BMW generation Otto-cycle motor. Performance and stability robustness of the control system are evaluated for a set of design specifications. Compensators are designed to eliminate rotation disturbances and improve oscillatory response. For both techniques, many design parameters are modified to compare their effectiveness. Despite system uncertainties, for most choices, the response is satisfactory. Thus, the influence of the choice of the technique and its parameters in a control design for a real application can be compared. Finally, compensator order is reduced to simplify its implementation.*

***Keywords****: Robust Control, Otto-cycle, LQG, H-∞*

## 1. INTRODUCTION

A robust system has to work satisfactorily when dynamics differs from the one considered during design. Despite small alterations in the dynamics, the system shall keep its stability and performance. The purpose of this paper is to study some changes in parameters for the LQG/LTR and H-∞ methods, two well known methods for the design of multivariable robust compensators. These methods aim at a compensator that satisfies a set of specifications for robust stability and performance. The present study addresses idle speed compensator design for an old generation BMW gasoline Otto-cycle motor (Geering, 1996). Such system is greatly affected by external disturbances and parameter changes (Kuraoka et al., 1990). In the next section, this system will be described and a mathematical model presented.

The LQG/LTR Method consists of a recovery process to match the closed-loop response with a desired dynamics. This method is described in section 3. In section 4, the H-∞ problem is described and its design specifications are chosen. The results are shown in section 5. After compensator design, it is possible to reduce its order, without compromising significantly the system response. In section 6, order reduction is used to get a simplified version of the compensator. Section 7 shows results obtained with the modified LQG/LTR compensator introduced by Prakash (1990). It is shown that the system has a good response for this less well known structure.

## 2. MATEMATICAL MODEL

Figure 1 shows the block diagram of the motor described in Kienitz (2006) based on Baumgartner et al. (1986) and Geering (1986). This diagram considers the dynamics of the fuel admission valve actuator, the flow and the rotation of the engine. Higher-order dynamics are not being considered. The process variable of interest is the engine's rotation ($\Delta n$). In this model, there are three manipulated variables: the reference for position of the fuel valve ($\Delta\alpha_r$), the ignition point ($\Delta\alpha_z$) and the time increment for opening fuel valve ($\Delta t_i$). The disturbance is the variation of the load from the default reference ($\Delta M_L$). For using state equations, the following states are being considered: position of the entrance valve ($\Delta\alpha_p$), pressure of the admission pipe ($\Delta p_S$) and rotation of the engine ($\Delta n$). The operating point and the parameters of the motor, which were used herein, can be seen in Tab. 1 and in Fig. 1.

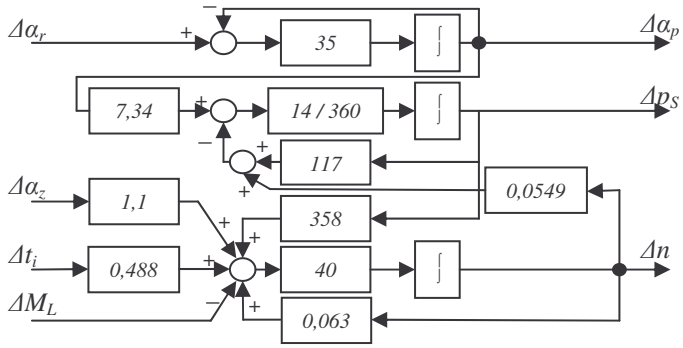


Figure 1. Linearized model of the motor

Table 1. Operating point of the Motor

| | | | |
|---|---|---|---|
| Rotation | n | 1000 | rpm |
| Load | M | 10 | Nm |
| Admission pressure | $p_s$ | 0,45 | Bar |
| Ignition point increment | $\alpha_z$ | 0 | Inkr $\alpha_z$ |
| Time increment of admission valve movement | $t_i$ | 0 | Inkr $t_i$ |

When a step disturbance of 40 Nm is applied in the load (i.e. the load jumps from 10 Nm to 50 Nm) motor rotation decreases from 1000 rpm to around 600 rpm. The response to this disturbance is seen in Fig. 2.

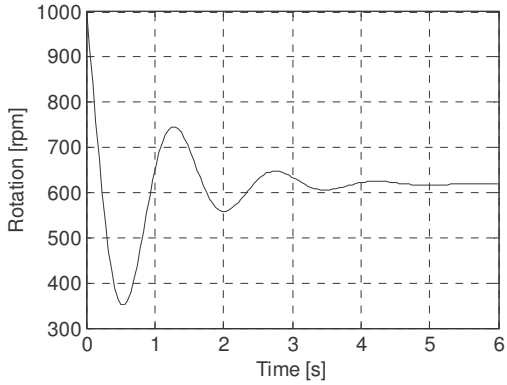


Figure 2. Response of the system to a step of 40 Nm in load

The main task of the compensator is to mitigate the influence of load disturbances on motor rotation. However, the ignition point and the time increment for opening the fuel valve should return to their initial (i.e. pre-transient) values. Therefore, to eliminate the disturbance, the dynamics of the system shall be increased by adding an integrator at the reference for position of the fuel valve. The integrator must not be added to other inputs, because these shall return to their initial values after the disturbance is compensated for. As a result, Equation (1) is obtained based on the model in Fig. 1.

$$\begin{cases} \dot{x} = Ax + BU + B_d \Delta M_L \\ y = Cx \end{cases} \tag{1}$$

Where

$$x = \begin{bmatrix} \Delta\alpha_p \\ \Delta P_S \\ \Delta n \\ \Delta\alpha_r \end{bmatrix} U = \begin{bmatrix} u \\ \Delta\alpha_Z \\ \Delta t_i \end{bmatrix} A = \begin{bmatrix} -35 & 0 & 0 & 35 \\ 0{,}2854 & -4{,}55 & -0{,}002135 & 0 \\ 0 & 14320 & 2{,}52 & 0 \\ 0 & 0 & 0 & 0 \end{bmatrix} B = \begin{bmatrix} 0 & 0 & 0 \\ 0 & 0 & 0 \\ 0 & 44 & 19{,}52 \\ 1 & 0 & 0 \end{bmatrix} B_d = \begin{bmatrix} 0 \\ 0 \\ -40 \\ 0 \end{bmatrix} C = \begin{bmatrix} 0 & 0 & 1 & 0 \end{bmatrix} \tag{2}$$

Instead of an integrator control, the use of PI-element that is shown in Eq. (3) is analyzed. In such case, only matrix *B* of Eq. (1) is modified. The new matrix *B* is given in Eq. (4).

$$\Delta\alpha_r = \left(0{,}2 + \frac{1}{s}\right) u \tag{3}$$

$$B = \begin{bmatrix} 7 & 0 & 0 \\ 0 & 0 & 0 \\ 0 & 44 & 19{,}52 \\ 1 & 0 & 0 \end{bmatrix} \tag{4}$$

## 3. LQG/LTR METHOD

The nominal system has no pole at the origin. Thus a compensator with an integral component is necessary to remove steady-state error for step disturbances. When an integrator or a PI element is added, the steady-state error is

eliminated. Furthermore it is also necessary to decrease settling time and overshoot. Additionally a main objective of the compensator is to keep stability robustness independently of reasonable modeling errors. The design specifications are shown in the next sections.

### 3.1. Stability robustness

The stability robustness specification depends on a modeling error assessment. The model given in Eqs. (1) and (2) describes a nominal system, $G_{nom}(s)$. In this case, a reasonable structure for the modeling error is shown in Eq. (5).

$$G(s) = [I + E(s)]G_{nom}(s) \tag{5}$$

Most of modeling errors are due to high-order dynamics neglected in the modeling process, such as actuator dynamics. A first order model of the neglected dynamics is given in Eq. (6).

$$G(s) = G_{nom}(s)\begin{bmatrix} 1/(1+T_1 s) & 0 & 0 \\ 0 & 1/(1+T_2 s) & 0 \\ 0 & 0 & 1/(1+T_3 s) \end{bmatrix} \tag{6}$$

Combing Eq. (5) and Eq. (6), the following error equation results:

$$E(s) = \begin{bmatrix} -T_1 s/(1+T_1 s) & 0 & 0 \\ 0 & -T_2 s/(1+T_2 s) & 0 \\ 0 & 0 & -T_3 s/(1+T_3 s) \end{bmatrix} \tag{7}$$

Cruz (1996) gives the condition for stability robustness shown in Eq. (8).

$$\sigma_{max}[G(j\omega)K(j\omega)] < 1/e_m(\omega), \forall \omega \tag{8}$$

where $e_m(\omega)$ is the upper limit given in Eq. (9) for the modeling error.

$$e_m(w) = \sigma_{max}[E(j\omega)] = \sigma_{max}\left[\frac{-T_{max}s}{1+T_{max}s}\right] \therefore T_{max} = max(T_1, T_2, T_3) \tag{9}$$

In this paper, we adopt $T_{max}$ = 0.02 seconds, i.e. the actuator reaches 99% of the desired value in less time than $5T_{max}$ (0.1 seconds). Then, the stability robustness condition is

$$\sigma_{max}[G(j\omega)K(j\omega)] < \frac{1+0{,}02s}{-0{,}02s} \tag{10}$$

### 3.2. Rejection of measurement noise

Most of the measurement noise is in the frequency of the motor rotation and its harmonics. Cruz (1996) proposes the following specification to guarantee noise rejection:

$$\sigma_{max}[G(j\omega)K(j\omega)] \leq \alpha_N(\omega) \tag{11}$$

The motor, whose nominal rotation is 1000 rpm, has a rotation frequency of $\omega = 2\pi(1000/60)$ rad/s = 104,7 rad/s. In this paper, an attenuation of -20dB in frequencies above rotation frequency was chosen, i.e. $\alpha_N(\omega)$ is equal to 0,1. This specification is shown in Fig. 4 as a dashed line as well as the specification from Eq. (10).

### 3.3. Target dynamics

The LQG/LTR method has two steps. In the first step a target (desired) dynamic is determined. In the second step, a compensator that forces this dynamic unto the actual feedback loop is designed. In Fig. 3, the structure of the admissible target dynamics is shown. Matrices $A$ and $C$ are used in this model and the issue is to find a matrix $H$ that entails a singular value diagram of $C\Phi(s)H$ that satisfies the specifications from Eq. (10) and Eq. (11).

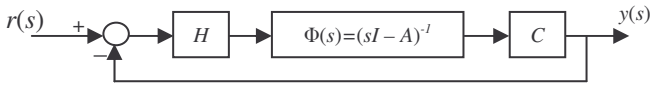


Figure 3. Target dynamics

The matrix $H$ is determined as the solution of a (fictitious) continuous time Kalman filter (Athans, 1986). The expression for calculating the filter gain matrix $H$ is

$$H = \frac{1}{\mu}\Sigma C^T \tag{12}$$

where $\Sigma$ is the solution of the algebraic Riccatti equation

$$A\Sigma + \Sigma A^T + LL^T - \frac{1}{\mu}\Sigma C^T C\Sigma = 0 \tag{13}$$

The design parameters are the matrix $L$ and the number $\mu > 0$. In this paper, the following choices for $L$ are considered: $B$, $aB$, $I$ and $aB + bI$, where $a$ and $b$ are constants, $I$ is a fourth order identity matrix and $B$ is the extended system input matrix. Figure 4 shows a singular value diagram of $C\Phi(s)H$ for each choice of $L$. Both dashed lines are specifications from Eq. (10) and Eq. (11). The first singular value diagram is plotted for the system shown in Eq. (2) plus an added integrator. The others are given for the system with an added PI-element of the type shown in Eq. (3). The gain values and the matrix L used in each case can be seen in the legend of Fig. (4). We can see that all graphics have the same shape, except for the identity matrix. This one decreases the effect of integral control in low frequencies.

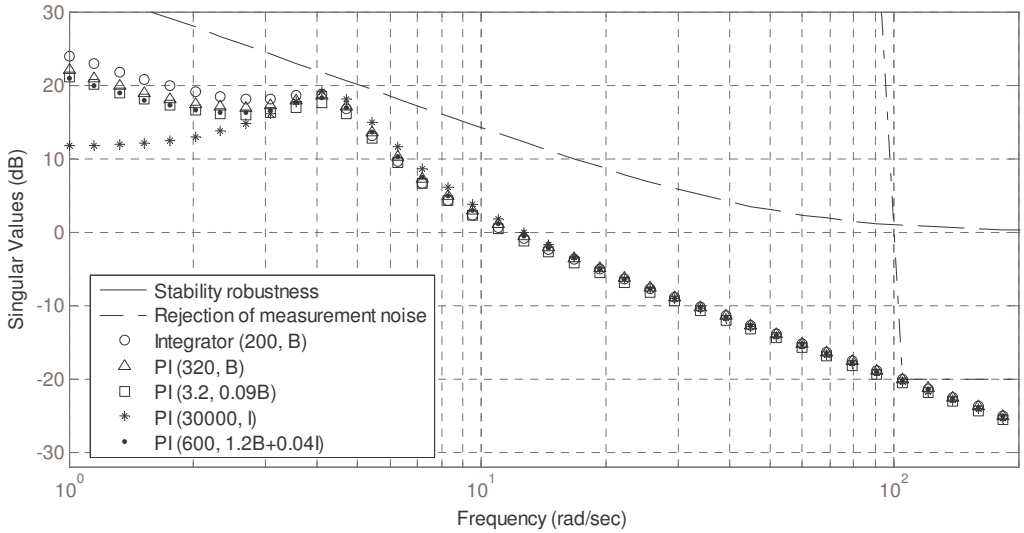


Figure 4. Singular value diagram of $C\Phi(s)H$ for each choice of $\mu$ and matrix $L$

### 3.4. Loop-Transfer-Recovery

In the Loop-Transfer-Recovery process, a compensator is designed to enforce the desired target dynamic. Figure 5 shows the structure of the controller. At this point matrices $A$, $B$, $C$ and $H$ are known. In this section, a matrix $G$ is determined via the solution of the Linear-Quadratic Regulator problem (Athans, 1986). Equation (14) presents the state equation for this structure.

$$\begin{cases} \dot{z} = Az + Bu + H(-e - Cz) \\ y = -Gz \end{cases} \tag{14}$$

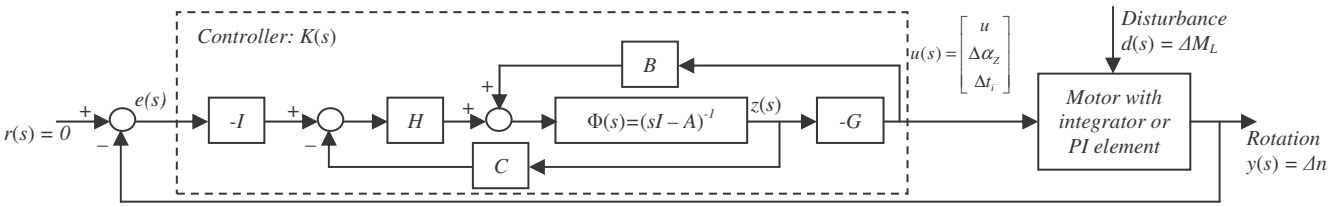


Figure 5. Compensator structure

We should solve the algebraic Riccatti equation in Eq. (15), and then compute the matrix *G* by using Eq. (16).

$$-KA - A^T K - C^T C + \frac{1}{\rho} KBB^T K = 0 \quad \therefore \rho \to 0^+ \tag{15}$$

$$G = \frac{1}{\rho} B^T K \tag{16}$$

As $\rho$ approximates to zero, the closed loop transfer function of the system tends to the closed loop transfer function of target dynamics shown in Fig. 3 (Athans, 1986). This happens whenever the system to be controlled does not have nonminimum phase zeros.

In Fig. 6, the target frequency response is given for $L = B$ and $\mu = 320$. The frequency response of the recovered system is also plotted for $\rho = 0{,}1$ and for $\rho = 0{,}01$. It is clearly seen that lower $\rho$ lead to better recovery.

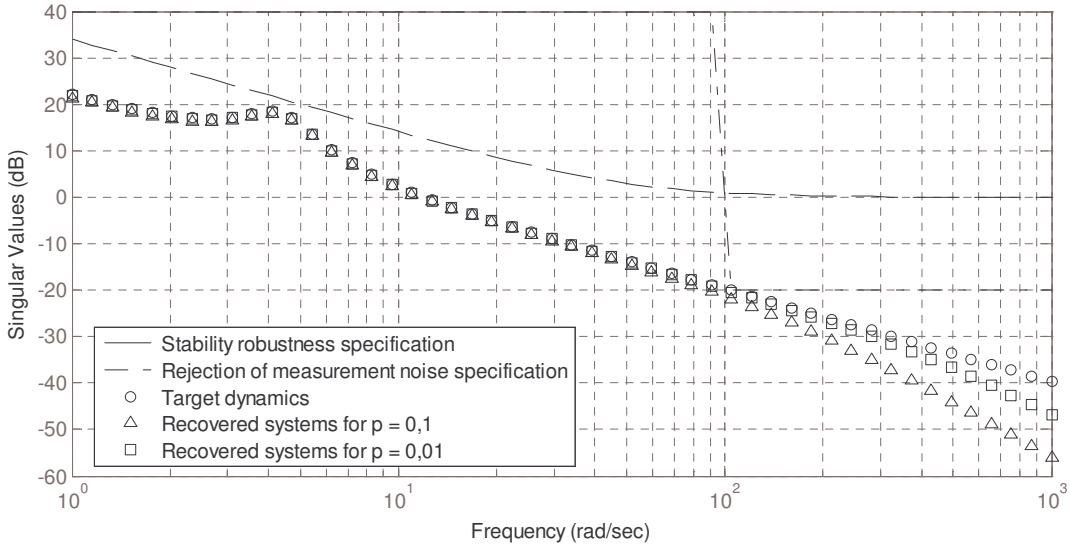


Figure 6. Singular value diagrams for the target and the recovered systems for $\rho = 0{,}1$ and $\rho = 0{,}01$.

## 4. H-∞ METHOD

To use H-∞ design, the system must be redrawn as shown in Fig. 7 (Levine and Reichert, 1990). The related equations are given in Eq. (17).

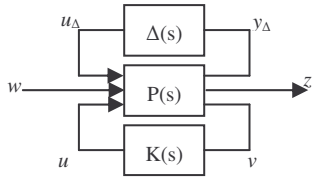


Figure 7. General structure of H-∞ problem, including modeling error

$$\begin{bmatrix} z \\ v \end{bmatrix} = P(s)\begin{bmatrix} w \\ u \end{bmatrix} = \begin{bmatrix} P_{11} & P_{12} \\ P_{21} & P_{22} \end{bmatrix}\begin{bmatrix} w \\ u \end{bmatrix} \tag{17}$$

In the H-∞ design, the controller $K$ is determined such that the infinity norm of the transfer function from input to output, $F(P, K)$ in Eq. (18), is minimized (Maciejowski, 1989).

$$z = F(P,K)w \therefore F(P,K) = P_{11} + P_{12}K(I - P_{22}K)^{-1}P_{21} \tag{18}$$

A diagram for matrix $P(s)$ is shown in Fig. 8. The inputs $w_1$, $w_2$ e $w_3$ are respectively represented by $u_\Delta$ (providing for $\Delta(s)$), $d(s)$ (disturbance) and $n(s)$ (measurement noise). The outputs $z_1$ e $z_2$ represent the input to the uncertainty block $\Delta(s)$ and the output of the system $y(s)$. Then, when minimizing $F(P,K)$, the influence of $u_\Delta$, $d(s)$ and $n(s)$ in the output of the system is minimized. Despite modeling errors $\Delta(s)$, this guarantees the stability of the system (Skogestad and Postlethwaite, 1996). For adjusting system performance, the weights $W_a$, $W_b$ e $W_c$ were added as shown in Fig. 8.

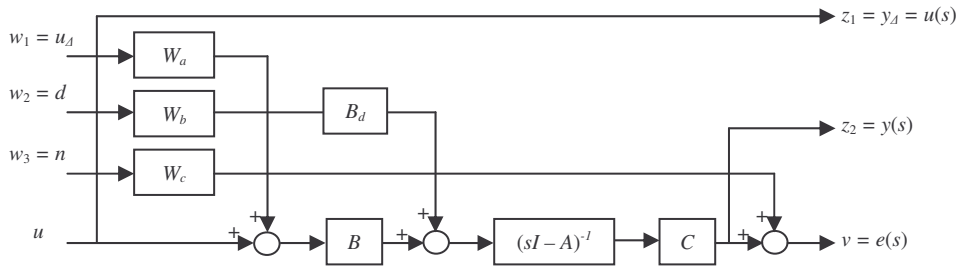


Figure 8. Diagram of matrix P(s)

The weight $W_a$ is chosen equal to the upper limit of the modeling error. This upper limit was determined in section 3.1 and is applied here, i.e. Equation (10) with $T_{max}$ equal to 0.02 is used to compute the weight $W_a$. This equation for $W_a$ is given in Eq. (19) where $\gamma_1$ is a design constant. In this case, the error $\Delta(s)$ is unknown but limited by $||\Delta(s)|| \leq 1$.

$$W_a = \frac{\gamma_1 T_{max} s}{T_{max} s + 1}[I_3] = \frac{\gamma_1 s}{s + 50}[I_3] \tag{19}$$

The weight $W_b$ is chosen as a low-pass filter function given in Eq. (20) where $\gamma_2$ and $b$ are design constants.

$$W_b = \frac{\gamma_2 b}{s + b} \tag{20}$$

The last weight $W_c$ is chosen as a high-pass filter that stops frequencies lower than the cutoff frequency. The cutoff frequency is adjusted considering the measurement noise spectrum. It was seen in section 3.2 that most of the measured noise is in the rotation frequency (104,7 rad/s) and its harmonics. This results in a choice of $W_c$ according to Eq. (21) where $\gamma_3$ and $b$ are design constants.

$$W_c = \frac{\gamma_3(s + b)}{s + c} = \frac{\gamma_3(s + b)}{s + 104{,}7} \tag{21}$$

Using Eq. (19), Eq. (20) and Eq. (21), the extended system $P(s)$ is described by the state equation in Eq. (23) with the following matrices.

$$\begin{cases} x = \begin{bmatrix} x_{4x1} \\ x_{\Delta 3x1} \\ x_{f1} \\ x_{f2} \end{bmatrix} w = \begin{bmatrix} u_\Delta(s) \\ d(s) \\ n(s) \end{bmatrix} z = \begin{bmatrix} u(s) \\ y(s) \end{bmatrix} A = \begin{bmatrix} A & B & B_d & 0 \\ 0 & -50I_3 & 0 & 0 \\ 0 & 0 & -b & 0 \\ 0 & 0 & 0 & -104{,}7 \end{bmatrix} B_1 = \begin{bmatrix} \gamma_1 B & 0 & 0 \\ -\gamma_1 50 I_3 & 0 & 0 \\ 0 & \gamma_2 b & 0 \\ 0 & 0 & -\gamma_3 104{,}7 + \gamma_3 b \end{bmatrix} B_2 = \begin{bmatrix} B \\ 0 \\ 0 \\ 0 \end{bmatrix} \\ C_1 = \begin{bmatrix} 0_{3x4} & 0_{3x3} & 0_{3x1} & 0_{3x1} \\ C & 0_{1x3} & 0 & 0 \end{bmatrix} C_2 = \begin{bmatrix} C & 0_{1x3} & 0 & 1 \end{bmatrix} D_{11} = \begin{bmatrix} 0_{3x3} & 0_{3x1} & 0_{3x1} \\ 0_{1x3} & 0 & 0 \end{bmatrix} D_{12} = \begin{bmatrix} I_3 \\ 0_{1x3} \end{bmatrix} D_{21} = \begin{bmatrix} 0_{1x3} & 0 & \gamma_3 \end{bmatrix} D_{22} = \begin{bmatrix} 0_{1x3} \end{bmatrix} \end{cases} \tag{22}$$

$$\begin{bmatrix} \dot{x} \\ z \\ v \end{bmatrix} = \left[\begin{array}{c|cc} A & B_1 & B_2 \\ \hline C_1 & D_{11} & D_{12} \\ C_2 & D_{21} & D_{22} \end{array}\right] \begin{bmatrix} x \\ w \\ u \end{bmatrix} \tag{23}$$

To apply H-∞ design, some conditions must be satisfied. First, ($A$, $B_2$) must be controllable and ($A$, $C_2$) observable. It is also necessary that the matrices in Eq. (24) have a full rank for any frequency. These conditions guarantee the existence of the H-∞ compensator. In section 2, an integral or PI control was added to eliminate the steady-state error. Because this new pole in the origin of complex axes, the matrices in Eq. (24) do not have full rank. To solve this problem, the imaginary axis was shifted a distance of $d$ (see Kienitz and Yoneyama, 1993 and references therein). After the design of the compensator, the imaginary axis is shifted back again. This results in suboptimality and the distance $d$ becomes a new design parameter.

$$\begin{bmatrix} A - jwI & B_2 \\ C_1 & D_{12} \end{bmatrix} \qquad \begin{bmatrix} A - jwI & B_1 \\ C_2 & D_{21} \end{bmatrix} \tag{24}$$

For performance tuning, the design parameters $\gamma_1$, $\gamma_2$, $\gamma_3$, $b$ and $d$ are used. The following values were found to be appropriate:

$$\gamma_1 = -0{,}1 \qquad \gamma_2 = 5 \qquad \gamma_3 = 0{,}005 \qquad b = 0{,}2 \qquad d = 0{,}05 \tag{25}$$

These parameters were used to compute the matrices in Eq. (22). Thereafter the compensator was found using the algorithm given by Safonov et al. (1989). This algorithm initially finds a suboptimum compensator that satisfies Eq. (26) for some value of γ. Then, the procedure is repeated reducing γ until the optimal compensator is found.

$$\left\| F(P,K) \right\|_\infty < \gamma \tag{26}$$

## 5. RESULTS

Figure 9 shows the step-disturbance responses resulting from the use of each compensator. The disturbance is a step of 40 Nm in motor load. It is observed that, except for response for $L = I$, all responses are correcting the disturbance effect returning to nominal rotation in reasonable time. Figure 10 presents the variation of position of the fuel valve ($\Delta\alpha_r$) for some compensators. We can see that this variable assumes a new operating point because of the disturbance. The variation of the ignition point ($\Delta\alpha_z$) and the time increment for opening fuel valve ($\Delta t_i$) for each compensator are illustrated in Fig. 11 and in Fig. 12. These variables return to zero after the effect of the disturbance is mitigated, as required in the problem formulation. Except for the case $L = I$, all controlled systems have better settling time than the response in Fig. 2 and a PI control produces a compensator with less oscillatory amplitude than an integral control, besides the least steady-state error. In the context of LQG/LTR method, comparing all responses, the best one happens when matrix $L$ is equal to $1{,}2B + 0{,}04\,I$, less settling time and less amplitude of transient than the others.

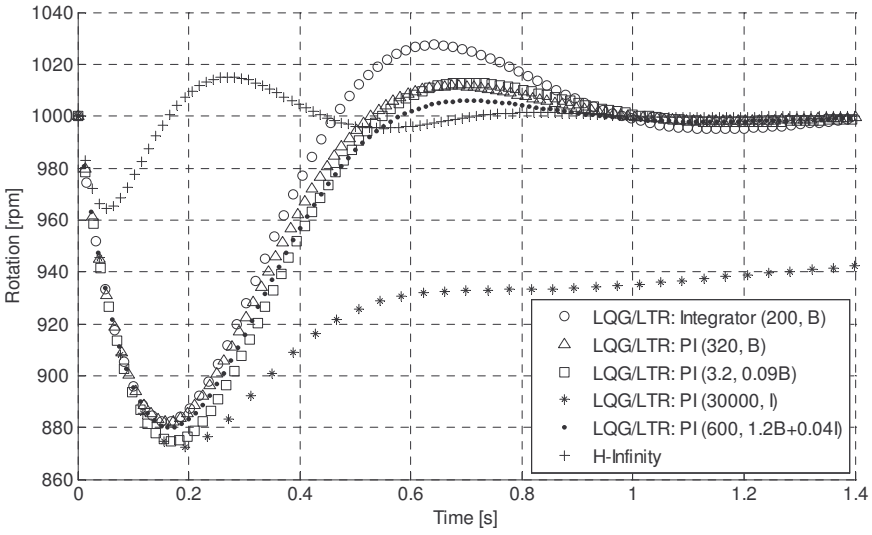


Figure 9. Step-disturbance responses for each compensator

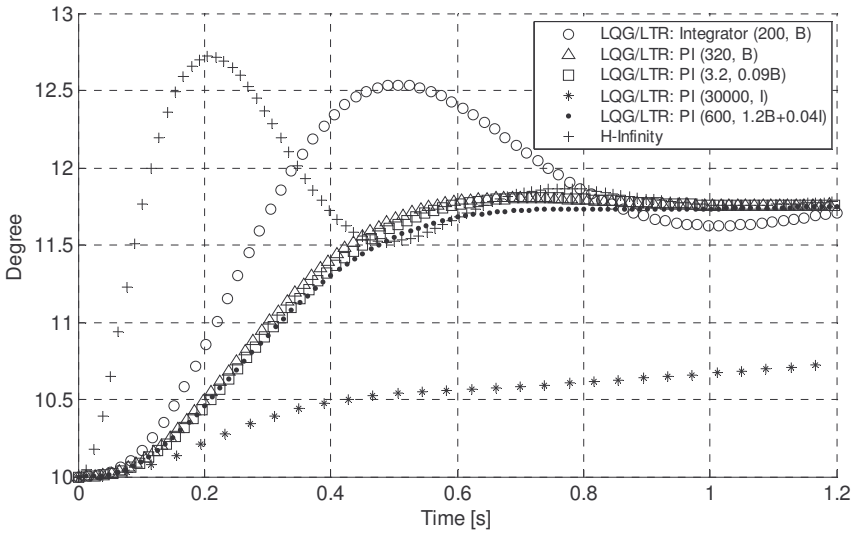


Figure 10. Variation of position of the fuel valve ($\Delta\alpha_p$) for each compensator

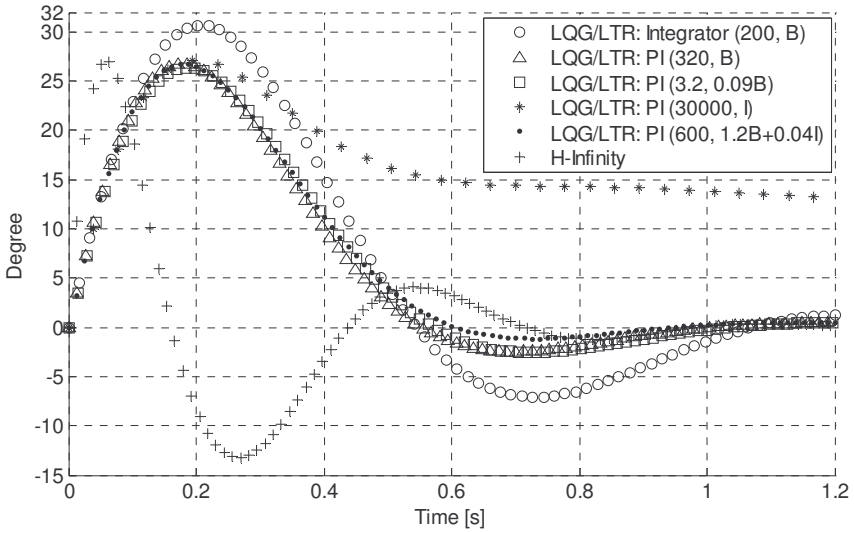


Figure 11. Variation of the ignition point ($\Delta\alpha_z$) for each compensator

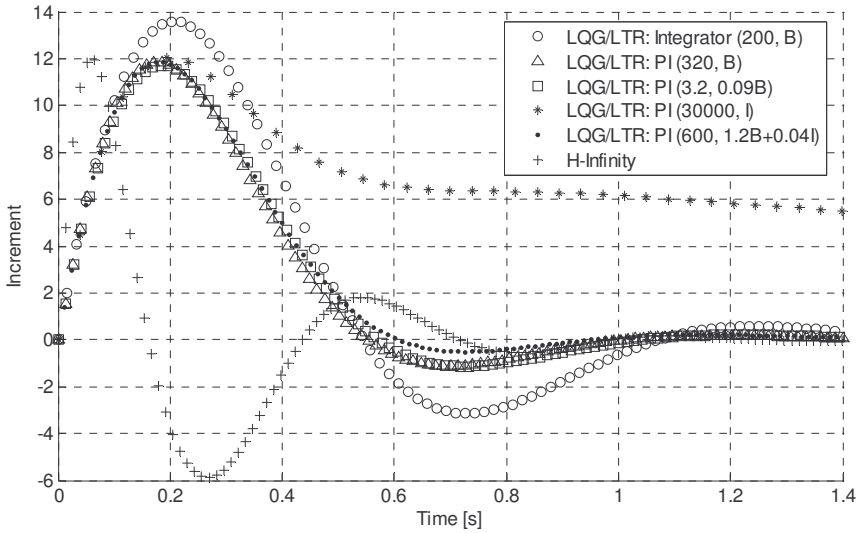


Figure 12. Time increment for opening fuel valve ($\Delta t_i$) for each compensator

## 6. ORDER REDUCTION

The LQG/LTR design produces a compensator with the same order as the extended system. Thus the third-order system extended with an integral or PI element produces a fourth-order LQG/LTR compensator. This results in an overall fifth-order controller. To have a simplified implementation, the order of controller can be reduced. This was done using a Matlab implementation of *Schur balanced truncation*. To assess the effect of order reduction, the best compensator was chosen, i.e. the compensator for $L = 1{,}2\ B + 0{,}04\ I$. During order reduction one state of the compensator was removed.

The H-∞ design produces a compensator with the order of $P(s)$, i.e. order 9 in this paper. Thus, the order of the compensator including the integrator or the PI element is ten. To have a simplified implementation, the order of compensator was reduced using the same algorithm mentioned before, *Schur balanced truncation*. The reduced compensator is of fourth order. Figure 14 shows the output for a step disturbance of 40 Nm in the load. The system shows satisfactory performance in both cases.

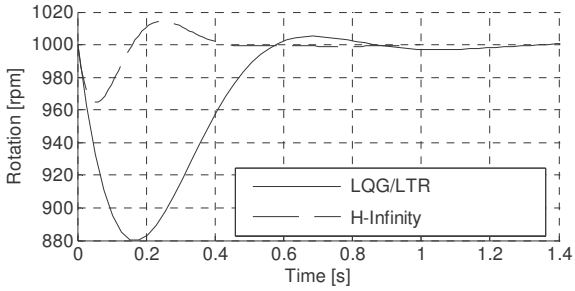


Figure 13. Step-disturbance responses for reduced and non-reduced compensator, using both methods.

## 7. NEW STRUCTURE FOR LTR

In Prakash (1990), an alternate control structure was introduced for LQG/LTR. Figure 14 shows this structure.

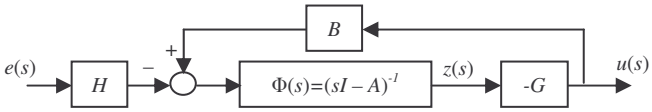


Figure 14. Prakash's structure

To compute the gain $G$, the process is the same that was used in section 3. The control transfer function still works inverting the dynamics of the system in Eq. (1). Equation (27) presents the state equation for this new structure.

$$\begin{cases} \dot{z} = Az + Bu - He(t) \\ y = -Gz \end{cases} \tag{27}$$

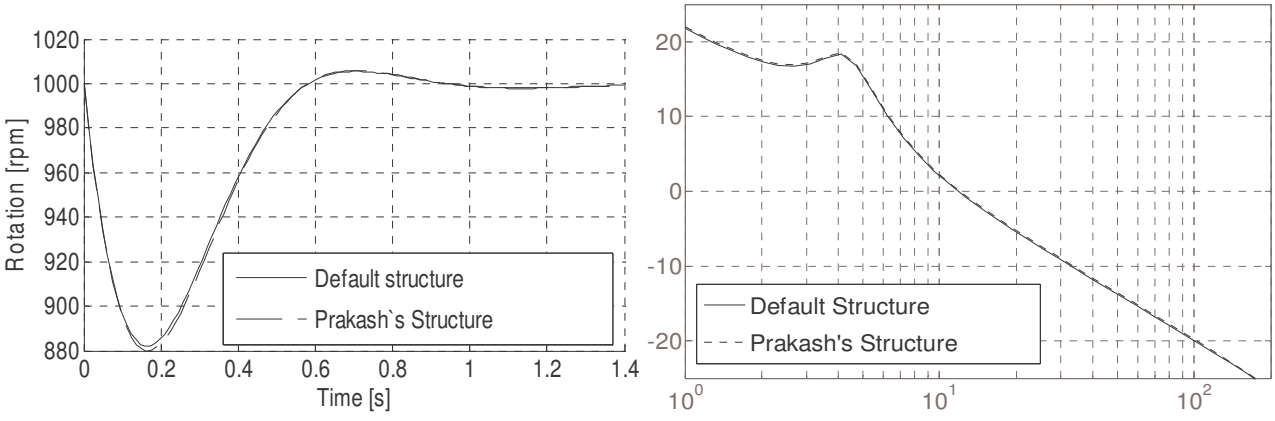


Figure 15. Step-disturbance responses and singular value diagram of the recovered system ($\rho = 0{,}01$) for default structure and for Prakash's structure.

Simulation results using this structure and the same step disturbance used in section 5 are summarized in Fig. 15. It also shows the singular value diagram of the recovered system for this structure and for the default structure, using $\rho = 0{,}01$. We can see that the new response is almost the same as the response of the default LQG/LTR structure. It was found in this application that the new structure leads to a stable compensator and a smaller LTR-Gain for recovery, corroborating the results published by Prakash (1990).

## 8. CONCLUSIONS

This work analyzed the LQG/LTR and H-∞ methods in an idle speed compensator design for an old generation BMW gasoline Otto-cycle motor. In this design, we evaluated the performance and stability robustness of the control system in the light of two simple but realistic design specifications. To satisfy the performance requirements in both methods, we attempt to maximize the closed-loop bandwidth without violating robustness stability requirements and without violating restriction of measurement noise rejection.

The influence of load disturbances on motor rotation was mitigated including an integrator at the reference for position of the fuel valve. However, the integrator was not added to other inputs, because these should return to their pre-transient values. Instead of an integrator control, we also tried the use of a PI element for the same purpose. We verified that, in this case, we reach less oscillatory response and less settling time than using a simple integrator.

In the context of the LQG/LTR method, the target dynamic with best performance (least transient amplitude and least settling time) was obtained for $L = 1{,}2\,B + 0{,}04\,I$.

When we compare the transient amplitude and the settling time in H-∞ and LQG/LTR methods, we observe that H-∞ design produces a compensator with better performance than LQG/LTR design. On the other hand, the H-∞ compensator is more complex than the LQG/LTR compensator. After controller reduction this difference in complexity is significantly reduced. We obtained a third order compensator from the LQG/LTR design and a fourth order one from the H-∞ design.

Prakash´s structure is less well known; it also led to a system with satisfactory response. This structure guarantees a stable compensator. The new structure also guarantees a smaller LTR-Gain for recovery that helps to avoid running into nonlinear actuator regions.

Finally, both methods show qualities and difficulties to design a controller that satisfy all robustness and performance requirements.

## 9. REFERENCES


Athans, M., 1986, “A Tutorial on LQG/LTR Method”, Proceedings of American Control Conference, Seattle, WA, USA, pp. 1289-1296.

Baumgartner, C.E. et al., 1986, "Robust multivariable idle speed control", Proceedings of the 1986 American Control Conference.

Cruz, J. J., 1996, “Controle Robusto Multivariável”, Edusp, S. Paulo, Brazil, 168 p.

Geering, H.P., 1986, "Entwurf robuster Regler mit Hilfe con Singularwerten: Anwendung auf Automobilmotoren", GMA-Bericht Nr. 11, Robuste Regelung, pp. 125-145.

Geering, H.P., 1996, “Regelungstechnik”, Springer, Berlin, Germany, 338p.

Kienitz, K.H., 2006, Private Communication, ITA, São José dos Campos, Brazil.

Kienitz, K.H. and Yoneyama, T., 1993, “A Robust Controller for Insulin Pumps Base Based on H-Infinity Theory”, IEEE Transactions on Biomedical Engineering, Vol. 40, No. 11, pp. 1133-1137.

Kuraoka, H., Ohka, N., Ohba, M., Hosoe, S. and Zhang, F., 1990, “Application of H-Infinity Design to Automotive Fuel Control”, IEEE Control Systems Magazine, Vol.10, No. 3, pp. 102-106.

Levine, W.S. and Reichert, R.T., 1990, “An Introduction to H∞ Control System Design”, Proceedings of the 29th Conference on Decision and Control, Vol.6, Honolulu, HI, USA, pp. 2966-2974.

Maciejowski, J.M., 1989, “Multivariable Feedback Design”, Addison-Wesley Publishing, Wokingham, England, 480 p.

Prakash, R., 1990, “Target Feedback Loop/Loop Transfer Recovery (TFL/LTR) Robust Control Design Procedures”, Proceedings of the 29th Conference on Decision and Control, Vol.3, Honolulu, HI, USA, pp 1203-1209.

Safonov, M. G., Limebeer, D. J. N. and Chiang, R. Y., 1989, "Simplifying the H-Infinity Theory via Loop Shifting, Matrix Pencil and Descriptor Concepts", Internacional Journal of Control, Vol.50, No. 6, pp. 2467-2488.

Skogestad, S. and Postlethwaite, I., 1996, “Multivariable Feedback Control”. John Wiley & Sons, England, 572 p.


## 10. RESPONSIBILITY NOTICE

The authors are the only responsible for the printed material included in this paper.